

## NUMERICAL SIMULATIONS OF WAVE SCATTERING FROM TWO-LAYERED ROUGH INTERFACE

**R. Wang and L.-X. Guo**

School of Science  
Xidian University  
No. 2, Taibai Road, Xi'an City, Shaanxi Province, China

**Abstract**—Method of Moments (MOM) combining with the Kirchhoff Approximation(KA) for analysis of the problem of optical wave scattering by a stack of two one-dimensional Gaussian rough interfaces is solved. The scattered field from the upper interface is solved by MOM and the transmitted field from the lower one is expressed from the Kirchhoff approximation where the multiple scattering phenomenon is neglected. The advantage of this hybrid method is that it is more exact than Kirchhoff approximation. The two rough interfaces separate three lossless and homogeneous media. The bistatic scattered field and the scattering coefficient are derived in this paper for vertical and horizontal polarizations. The influence of the relative permittivity, the height rms and the correlative length, the average heights between the two interfaces on the bistatic scattering coefficient is discussed in detail. The application of this work is the study of electromagnetic modeling of oil slicks on ocean surfaces.

### 1. INTRODUCTION

The study of electromagnetic/optical wave scattering from rough layered structures has been the subject of intensive investigation for its application in a number of important research areas [1–6], such as the remote sensing, either by radar or optical imagery, ocean engineering, the design of optical scanning instrument for use in the semiconductor industry as well as the surface optics. The remote sensing can be used for detection and monitoring of possible oil spill on ocean surfaces. However, other phenomena may lead to the same effects on measurements. Electromagnetic modeling of oil slicks could be an efficient mean to discriminate oil from lookalikes. In order to validate such environmental alterations on measurements, we focus on

the study of waves scattering from rough surfaces, in microwaves as well in optics domains. Electromagnetic models [7] for rough surfaces scattering have been developed for several years; however, these models generally consider only a single layer [8, 9], that is to say one rough interface. Their extension to multilayer separated by rough interfaces have been studied analytically [10, 11]; In this paper, we are interested in a numerical approach, using the hybrid method combining Method of Moments (MOM) with the first-order Kirchhoff approximation (KA) where the multiple scattering phenomenon is neglected. In this work, the considered multilayer consists of two one-dimensional Gaussian rough interfaces. The KA is used for the calculation of the transmitted field from the lower rough surface and the MOM for the calculation of the scattered field from the upper rough surface due to the incident field. We consider both the transverse magnetic (VV) and transverse electric (HH) solution to the hybrid method. The paper is organized as follows: the theoretical formulation of method of moments is firstly developed, and the transmitted fields from lower surface is derived using the Kirchhoff approximation [12–15], then the numerical results on the scattering coefficient of the two-layer model are given and discussed.

## 2. THE THEORETICAL FORMULA FOR THE SCATTERING MODEL

According to Fig. 1, the considered multilayer consists of two one-dimensional Gaussian rough interfaces. The upper one  $S_0$ , separates a lossless homogeneous dielectric medium  $\Omega_0(\varepsilon_0, \mu_0)$ , with relative permittivity  $\varepsilon_0 = 1$  and permeability  $\mu_0 = 1$ , from a lossless medium  $\Omega_1(\varepsilon_1, \mu_1 = \mu_0)$ . This homogeneous medium fills a layer separated from the semi-infinite lower medium  $\Omega_2(\varepsilon_2, \mu_2 = \mu_0)$  by another rough

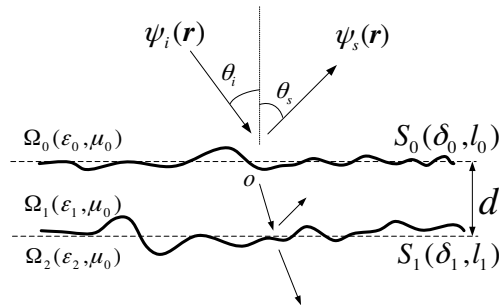


**Figure 1.** Geometric model of a stack of two one-dimensional Gaussian rough interfaces.

surface  $S_1$ . Each boundary is invariant with respect to any translation along the  $y$  axis. The height profiles of  $S_0$  and  $S_1$  are given by  $z_0 = f_0(x)$  and  $z_1 = f_1(x)$  respectively.  $d$  is the average height between the two Gaussian rough interfaces.

For the case of a two media problem where the lower medium ( $\Omega_1$ ) has permittivity  $\varepsilon_1$ , the dual integral equation is needed. Let  $\psi_0(\mathbf{r})$ ,  $\psi_1(\mathbf{r})$  be the field in  $\Omega_0$  and  $\Omega_1$ , respectively. The fields in  $\Omega_0$  and  $\Omega_1$  satisfy the following equations:

$$\psi_i(\mathbf{r}) = \frac{1}{2}\psi_0(\mathbf{r}) - \int_{P,V} ds \psi_0(\mathbf{r}') \hat{\mathbf{n}} \cdot \nabla G_0(\mathbf{r}, \mathbf{r}') + \int_s ds G_0(\mathbf{r}, \mathbf{r}') \hat{\mathbf{n}} \cdot \psi_0(\mathbf{r}') \quad (1)$$

$$\frac{1}{2}\psi_1(\mathbf{r}) + \int_{P,V} ds \psi_1(\mathbf{r}') \hat{\mathbf{n}} \cdot \nabla G_1(\mathbf{r}, \mathbf{r}') - \int_s ds G_1(\mathbf{r}, \mathbf{r}') \hat{\mathbf{n}} \cdot \nabla \psi_1(\mathbf{r}') = 0 \quad (2)$$

Note that  $G_0(\mathbf{r}, \mathbf{r}')$  and  $G_1(\mathbf{r}, \mathbf{r}')$  are the Green's functions for  $\Omega_0$  and  $\Omega_1$ , respectively.

$$G_0(\mathbf{r}, \mathbf{r}') = \frac{i}{4} H_0^{(1)}(k_0 |\mathbf{r} - \mathbf{r}'|), \quad G_1(\mathbf{r}, \mathbf{r}') = \frac{i}{4} H_0^{(1)}(k_1 |\mathbf{r} - \mathbf{r}'|) \quad (3)$$

where  $\mathbf{r}$  is on the rough surface. The field  $\psi_0(\mathbf{r})$ ,  $\psi_1(\mathbf{r})$  satisfies the following equation based on boundary condition:

$$\psi_0(\mathbf{r}) = \psi_1(\mathbf{r}) | \mathbf{r} \in S_0 \quad (4)$$

$$\hat{\mathbf{n}} \cdot \nabla \psi_0(\mathbf{r}) = \frac{\varepsilon_0}{\varepsilon_1} \hat{\mathbf{n}} \cdot \nabla \psi_1(\mathbf{r}) | \mathbf{r} \in S_0 \quad (5)$$

where the normal vector on the rough surface  $\hat{\mathbf{n}} = -\frac{f'}{\sqrt{1+f'^2}}\hat{x} + \frac{1}{\sqrt{1+f'^2}}\hat{z}$ . The rough surface is discretized along the  $x$  axis and MOM with point-matching is used. We can obtain the matrix equation from (1)–(2) as follows [16]:

$$\begin{bmatrix} A & B \\ C & \rho D \end{bmatrix} \cdot \begin{bmatrix} V_1(x) \\ V_2(x) \end{bmatrix} = \begin{bmatrix} \psi_i(x) \\ 0 \end{bmatrix} \quad (6)$$

where  $V_1(x) = \psi_0(\mathbf{r}) | \mathbf{r} \in S_0$ ,  $V_2(x) = u(x) = \sqrt{1 + (\frac{df_0}{dx})^2} (\hat{\mathbf{n}} \cdot \nabla \psi_0(\mathbf{r})) | \mathbf{r} \in S_0$ ,  $\rho = \varepsilon_1/\varepsilon_0$  for vertical polarization. The elements

of the matrix are shown below [17]:

$$A_{mn} = \begin{cases} \Delta x \kappa(x_m, x_n) & m \neq n \\ \frac{i\Delta x}{4} \left[ 1 + \frac{i2}{\pi} \ln \left( \frac{\gamma k_0}{4e} \Delta l_m \right) \right] & m = n \end{cases} \quad (7a)$$

$$B_{mn} = \begin{cases} -\Delta x \kappa_N(x_m, x_n) & m \neq n \\ \frac{1}{2} - \frac{f_0''(x_m)}{4\pi} \frac{\Delta x}{1 + (f_0'(x_m))^2} & m = n \end{cases} \quad (7b)$$

$$C_{mn} = \begin{cases} \Delta x \kappa_1(x_m, x_n) & m \neq n \\ \frac{i\Delta x}{4} \left[ 1 + \frac{i2}{\pi} \ln \left( \frac{\gamma k_1}{4e} \Delta l_m \right) \right] & m = n \end{cases} \quad (7c)$$

$$D_{mn} = \begin{cases} -\Delta x \kappa_{1N}(x_m, x_n) & m \neq n \\ -\frac{1}{2} - \frac{f_0''(x_m)}{4\pi} \frac{\Delta x}{1 + (f_0'(x_m))^2} & m = n \end{cases} \quad (7d)$$

where  $\Delta l_m = \Delta x \sqrt{1 + (f_0'(x_m))^2}$ ,  $\gamma = 1.78107$ ,  $e = 2.71828138$  and the wave number of  $\Omega_0$  and  $\Omega_1$  are  $k_0 = \omega \sqrt{\mu_0 \varepsilon_0}$ ,  $k_1 = \omega \sqrt{\mu_1 \varepsilon_1}$ , respectively.  $f_0'(x)$  and  $f_0''(x)$  are the first- and second-order differential of rough surface height function, respectively, and the detail expressions of  $\kappa$ ,  $\kappa_N$ ,  $\kappa_1$ ,  $\kappa_{1N}$  are given in [15]. After solving the matrix Eq. (5), we can obtain the  $\psi_0(\mathbf{r})$  and  $\hat{\mathbf{n}} \cdot \nabla \psi_0(\mathbf{r})$  without considering the transmitted field from  $\Omega_1$ . In order to calculate the total field  $\psi(\mathbf{r})$  of every point on the upper rough surface  $S_0$  with considering the transmitted field  $\psi_{10}^{tr}(\mathbf{r})$ , it is necessary to derive the value of the transmitted fields  $\psi_{10}^{tr}(\mathbf{r})$  of every point. In the following, the Kirchhoff approximation is applied to derive the transmitted fields. The transmitted fields  $\psi_{10}^{tr}(\mathbf{r}_2)$  into  $\Omega_0$  at the points  $C(\mathbf{r}_2)$  due to the rough upper and lower interfaces is calculated, as represented in Fig. 2.

We consider that the upper and lower rough surfaces have on every point a large radius of curvature relative to the wavelength of the incident fields,  $\lambda_0$  and  $n_1 \lambda_0$ , respectively,  $n_1$  being the index of refraction in  $\Omega_1$ . Under the condition, the tangent plane hypothesis is valid and Fresnel laws can be locally applied. Thus, at the point  $A(\mathbf{r}_0)$  on  $S_0$ , we consider the transmitted light  $\psi_{01}^{tr}$ . The transmitted field  $\psi_{01}^{tr}$  into  $\Omega_1$  due to the incident field  $\psi_i(\mathbf{r}_0)$  is by

$$\psi_{01}^{tr}(\mathbf{r}_0) = T_{01}(\mathbf{r}_0) \psi_i(\mathbf{r}_0) \quad (8a)$$

$$\hat{\mathbf{n}}_0 \cdot \nabla \psi_{01}^{tr}(\mathbf{r}_0) = T_{01}(\mathbf{r}_0) \frac{\partial \psi_i(\mathbf{r}_0)}{\partial n_0} \quad (8b)$$

where  $T_{ij} = \rho_{ij}(1 + R_{ij})$  is the Fresnel transmission coefficient. For horizontal polarization  $\rho_{ij} = 1$  and for vertical polarization  $\rho_{ij} =$

$$R_{ij}(\vec{r}) = \begin{cases} \frac{\cos \theta_k - (\varepsilon_j/\varepsilon_i - \sin^2 \theta_k)^{1/2}}{\cos \theta_k + (\varepsilon_j/\varepsilon_i - \sin^2 \theta_k)^{1/2}} & \text{for horizontal polarization} \\ \frac{\varepsilon_j/\varepsilon_i \cos \theta_k - (\varepsilon_j/\varepsilon_i - \sin^2 \theta_k)^{1/2}}{\varepsilon_j/\varepsilon_i \cos \theta_k + (\varepsilon_j/\varepsilon_i - \sin^2 \theta_k)^{1/2}} & \text{for vertical polarization} \end{cases} \quad (9)$$

and  $\varepsilon_{i(j)}$  is the relative permittivity of the medium  $\Omega_{i(j)}$  and  $\theta_{k=0,1,2}$  represents the local incidence angle as it is shown in Fig. 2. The transmitted beam from  $A(\mathbf{r}_0)$  will intercept the lower interface at point  $B(\mathbf{r}_1)$ . It can be easily located with the Fresnel law:

$$\sin \theta'_0 = \sin \theta_0 \frac{1}{\sqrt{\varepsilon_1}} \quad (10)$$

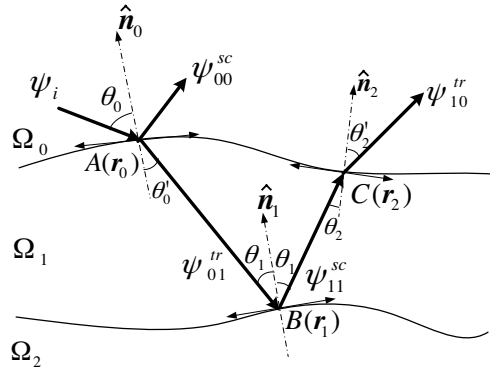


**Figure 2.** Kirchhoff approximation.

Finally, the transmitted field  $\psi_{10}^{tr}(\mathbf{r}_2)$  at  $C$  are [12]

$$\psi_{10}^{tr}(\mathbf{r}_2) = T_{10}(\mathbf{r}_2)R_{12}(\mathbf{r}_1)T_{01}(\mathbf{r}_0)\psi_i(\mathbf{r}_0)e^{-jk\sqrt{\varepsilon_1}(|\vec{r}_2-\vec{r}_1|+|\vec{r}_1-\vec{r}_0|)} \quad (11a)$$

$$\hat{\mathbf{n}}_2 \cdot \nabla \psi_{10}^{tr}(\mathbf{r}_2) = T_{10}(\mathbf{r}_2)(-R_{12}(\mathbf{r}_1))T_{01}(\mathbf{r}_0)\frac{\partial \psi_i(\mathbf{r}_0)}{\partial n_0}e^{-jk\sqrt{\varepsilon_1}(|\vec{r}_2-\vec{r}_1|+|\vec{r}_1-\vec{r}_0|)} \quad (11b)$$

In order to find the transmitted fields  $\psi_{10}^{tr}(\mathbf{r})$ , the phase shift between the field in  $A(\mathbf{r}_0)$  and  $C(\mathbf{r}_2)$  should be obtained. It is necessary

to determine numerically the locations of the points  $B$  and  $C$  for each point  $A(\mathbf{r}_0)$ . It is easy for us to obtain the numerical point  $B_{num}$  and  $C_{num}$  using some simple method. Finally,  $\Delta\varphi$  is estimated by [12]

$$\Delta\varphi = k\sqrt{\varepsilon_1}(AB_{num} + B_{num}C_{num}) \quad (12)$$

Then we can get  $\psi_{10}^{tr}(\mathbf{r})$  and  $\hat{\mathbf{n}} \cdot \nabla\psi_{10}^{tr}(\mathbf{r})$  for each point from Eq. (11). After obtaining  $\psi_0(\mathbf{r})$  and  $\hat{\mathbf{n}} \cdot \nabla\psi_0(\mathbf{r})$  with MOM. Finally, the values  $\psi_0(\mathbf{r})$  and  $\psi_{10}^{tr}(\mathbf{r})$  (if it exists) are added at each point of  $S_0$ , the total fields of each point of  $S_0$  is

$$\psi(\mathbf{r}) = \psi_0(\mathbf{r}) + \psi_{10}^{tr}(\mathbf{r}) \text{ if exist} \quad (13)$$

Notice that we calculate the Eq. (13) is to trace the ray reflected from the lower surface which means that in some regions of the upper surface there may be high density of such rays and other regions will have low density. This may be mainly due to the fact that in this paper, we are interested in the one-order Kirchhoff approximation where the multiple scattering phenomenon is neglected and to reduce the complexity of the hybrid method, the subsequent interactions between the two surfaces are ignored. Furthermore, these factors may introduce an error in the calculations especially for the calculation of the very rough layers. For the scattering computation, the two-layer surface realizations are needed at a set of  $P$  points with spacing  $\Delta x$  over length  $L = P\Delta x$ . Realizations with the desired properties can be generated at points  $x_p = p\Delta x (p = 1, \dots, P)$  using [14]

$$f_{0,1}(x_p) = \frac{1}{L} \sum_{i=-\frac{P}{2}}^{\frac{P}{2}-1} F(K_i) \exp(jK_i x_p) \quad (14)$$

where  $f_{0,1}(x_p)$  represents the height profiles of  $S_0$  and  $S_1$ , respectively. For  $i \geq 0$ ,

$$F(K_i) = \sqrt{2\pi LW(K_i)} \begin{cases} [N(0,1) + jN(0,1)]/\sqrt{2} & i \neq 0, P/2 \\ N(0,1) & i = 0, P/2 \end{cases} \quad (15)$$

and, for  $i < 0$ ,  $F(K_i) = F(K_{-i})^*$ .  $K_i = 2\pi i/L$  and each time  $N(0,1)$  appears, which indicates an independent sample taken from a zero mean, unit variance Gaussian distribution. For the present work, the rough surface model used in scattering model is generated randomly with a Gaussian roughness spectrum, i.e., [14]

$$W(K_i) = (l_{0,1}\delta_{0,1}^2/2\sqrt{\pi}) e^{-K_i^2 l_{0,1}^2/4} \quad (16)$$

where  $\delta_{0,1}$  represents the rms height of the upper and lower surface ( $S_0$  and  $S_1$ ), respectively as well as the correlation length  $l_{0,1}$ . Eq. (14) is computed with a fast Fourier transform (FFT). We can choose different values of the parameters ( $\delta_{0,1}$  and  $l_{0,1}$ ) for upper and lower Gaussian rough surface.

It should be noted that, in numerical simulation of scattering from rough surface, the tapered wave described by the tapering parameter  $g$  has been employed to guard against the edge effects associated with the illuminated finite surface  $L$ . The tapered incident wave illuminating the composite model is given by [17]

$$\psi_i(\mathbf{r}) = \exp(-jk_0(x \sin \theta_i - z \cos \theta_i)(1 + w(\mathbf{r}))) \exp\left(-\left(\frac{x + z \tan \theta_i}{g}\right)^2\right) \quad (17)$$

where  $g$  is the tapering parameter,  $\theta_i$  is the incident angle. The additional factor in the phase,  $w(\mathbf{r})$  is inserted such that  $\psi_i(\mathbf{r})$  obeys the wave equation to a higher order. The choice of  $w(\mathbf{r})$  is expressed as

$$w(\mathbf{r}) = \frac{\left[2\left(\frac{x + y \tan \theta_i}{g}\right)^2 - 1\right]}{(kg \cos \theta_i)^2} \quad (18)$$

Then we can write the analytical expression of the scattered field due to the rough upper and lower interfaces using Huygens's principle ( $\psi(\mathbf{r}_0)$  represents the total field on  $S_0$ )

$$\psi_s(\mathbf{r}) = \int_{S_0} [\psi(\mathbf{r}_0) \hat{\mathbf{n}} \cdot \nabla G_0(\mathbf{r}, \mathbf{r}_0) - G_0(\mathbf{r}, \mathbf{r}_0) \hat{\mathbf{n}} \cdot \psi(\mathbf{r}_0)] ds_0 \quad (19)$$

The bistatic RCS  $\sigma(\theta_s)$  in the direction  $\mathbf{k}_s$  is then calculated on the far field as in [17]:

$$\sigma(\theta_s) = \frac{|\psi_s^{(N)}|^2}{8\pi kg \sqrt{\pi/2} \cos \theta_i \left[1 - \frac{1 + 2 \tan^2 \theta_i}{2k^2 g^2 \cos^2 \theta_i}\right]} \quad (20)$$

with

$$\psi_s^{(N)} = \int_{-\infty}^{\infty} dx \left\{ \hat{\mathbf{n}} \cdot \nabla \psi \Big|_{z=f_0(x)} \sqrt{1 + f_0'(x)^2} - \psi(x) ik [f_0'(x) \sin \theta_s - \cos \theta_s] \right\} \cdot \exp[-ik(\sin \theta_s x - f_0(x) \cos \theta_s)] \quad (21)$$

### 3. NUMERICAL RESULTS AND DISCUSSIONS

In all the following numerical implementations, both the relevant parameters of the Gaussian rough surface are measured in incident wavelength  $\lambda$  and the rough surface is created by 100 Monte Carlo realizations in the following numerical simulations. The average height between the two interfaces is  $d = 5\lambda$  for the scattering plots in Fig. 3–6.

In the Fig. 3(a), We first illustrate the rough surface scattering from a two-layered Gaussian rough interfaces with the same parameters by the hybrid method and KA. The bistatic scattering coefficient of this two-layered Gaussian rough surface are computed by using the classical KA and the hybrid method, respectively. It is found that the scattering pattern by the hybrid method is in good agreement with that by KA near the specular angular range and there is great difference in the larger scattering angles. This indicates that the hybrid method is more exact than KA. We next illustrate in Fig. 3(b) rough surface scattering from a single- and two-layered system with Gaussian rough interfaces with the same parameters. It is easy for us to find that the bistatic scattering coefficient from two-layered system is larger than that from the single-layered system on the most scattering angles except for the specular direction. For the plot 1 in Fig. 3(b), the computing time of the numerical simulations is 65 s. Here, the rough surface is created by 1 Monte Carlo realization and the dominant frequency of CPU is 1.4 GHz.

To further explore the important scattering characteristic of the two-layer Gaussian rough surface model, the dependency of the bistatic scattering coefficient on relative permittivity  $\varepsilon_2$  is plotted for horizontal polarization by the hybrid algorithm in Fig. 4. The incident angles are  $\theta_i = 20^\circ$ . The height rms of the upper and lower rough surface are  $0.1\lambda$  and the correlative length  $1.2\lambda$ , respectively. It is observed that the bistatic scattering cross section of layered model increases with increasing  $\varepsilon_2$ . It should be pointed out that as for the case of  $\varepsilon_2 = \varepsilon_1$ , the two-layer media can be regarded as the single-layer media, and the total scattered field in  $\Omega_0$  only corresponds to the scattered field  $\psi_{00}^{sc}(\mathbf{r}_0)$  in  $S_0$  due to the incident field. As for the case of  $\varepsilon_2 \neq \varepsilon_1$  is concerned, the total scattered fields in  $\Omega_0$  consists of  $\psi_{00}^{sc}(\mathbf{r}_0)$  in  $S_0$  and  $\psi_{10}^{tr}(\mathbf{r})$  due to  $S_1$ , which results that the bistatic scattering coefficient of layered model increases with the larger value of the relative permittivity  $\varepsilon_2$  in the lower media.

In Fig. 5, the effect of the height rms on the bistatic scattering coefficient of the two-layer Gaussian rough surface with the same parameters ( $\delta_0 = \delta_1$ ,  $l_0 = l_1$ ) is examined. The incident angles are  $\theta_i = 5^\circ$ . The relative permittivity of  $\Omega_1$  and  $\Omega_2$  are  $\varepsilon_1 = 2.5$ ,  $\varepsilon_2 = 3.0$ ,

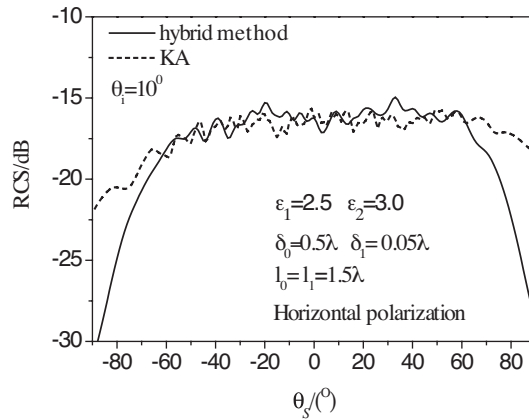


**Figure 3a.** Comparison of the hybrid method and KA for the two-layer model.

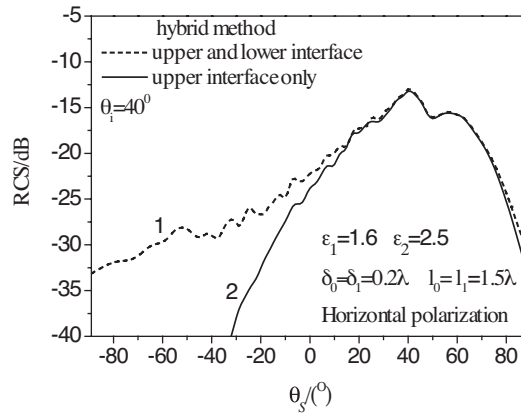


**Figure 3b.** The bistatic scattering coefficient of the single and two-layer model.

respectively. The correlative length is  $1.5\lambda$ . It is observed that the bistatic scattering coefficient increases with increasing  $\delta$  over the most angular range except for the specular direction. It is mainly due to the fact that the two-layer rough surface can be regarded as two flat interfaces for the small value height rms, which results in the obvious peaks on the specular direction (corresponding to the strong coherent scattering) and weak incoherent scattering in the angular range far from the specular direction.

In Fig. 6, the influence of the correlative length on the bistatic

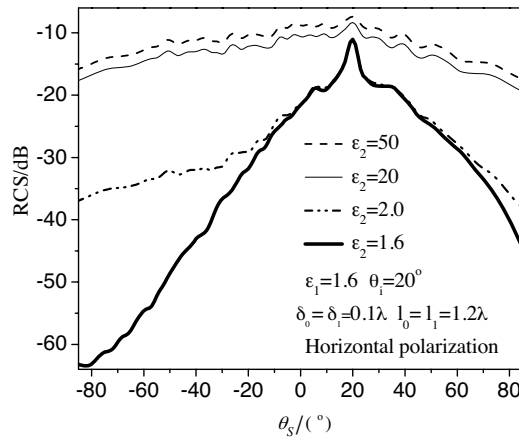


**Figure 4.** The bistatic scattering coefficient of the two-layer model versus  $\epsilon_2$ .

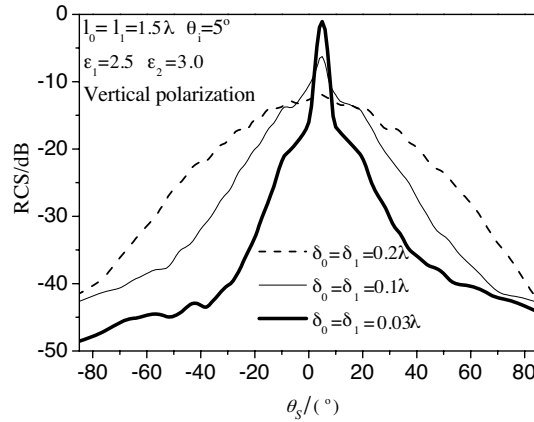


**Figure 5.** The bistatic scattering coefficient of the two-layer model versus  $\delta$ .

scattering coefficient of the two-layer Gaussian rough surface with the same parameters ( $\delta_0 = \delta_1$ ,  $l_0 = l_1$ ) for horizontal polarization is depicted. The incident angles are  $\theta_i = 10^\circ$ . The relative permittivity of  $\Omega_1$  and  $\Omega_2$  are as same as ones in Fig. 5. The rms height of  $S_0$  and  $S_1$  are both  $0.2\lambda$ . It can be seen that the bistatic scattering coefficient increases by keeping the rms height constant and by decreasing the correlation length, the electromagnetic roughness is constant, but the rms slope increases, leading to a higher angular spreading of the

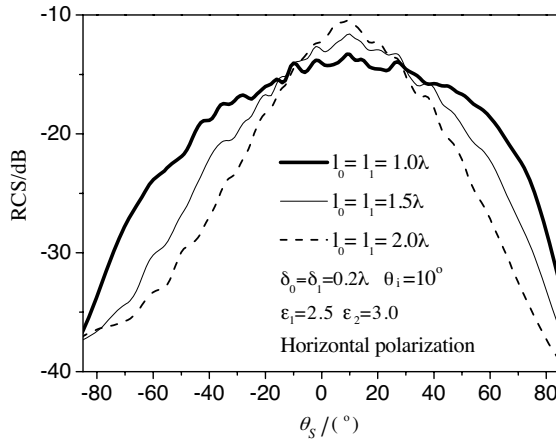


**Figure 6.** The bistatic scattering coefficient of the two-layer model versus  $l$ .

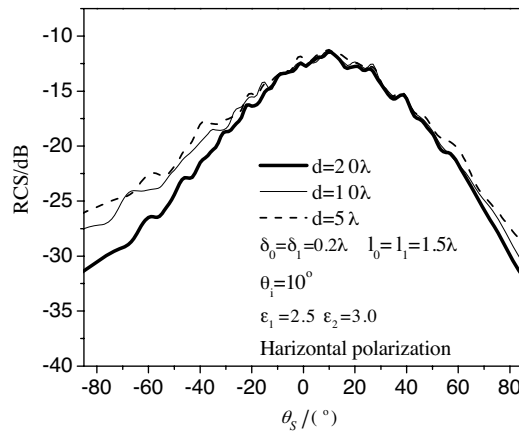


**Figure 7.** The bistatic scattering coefficient of the two-layer model versus  $d$ .

scattered energy. This implies a decrease of the scattered energy in the specular direction and a increase of the incoherent scattering (the heavy line shown as in Fig. 6). The rough surface scattering from two-layered system with the different heights  $d$  between the two interfaces for horizontal polarization are also present in Fig. 7. The height rms of the upper and lower rough surface are both  $0.3\lambda$  and the correlative length  $1.5\lambda$ , respectively. The incident angle is  $\theta_i = 10^\circ$  and the relative permittivity of  $\Omega_1$  and  $\Omega_2$  are as same as those in Fig. 6. It is found

that the bistatic scattering coefficient is not sensitive to the varying of the average height between the two interface.

#### 4. CONCLUSION

To investigate the bistatic scattering from a stake of two one-dimensional Gaussian rough surface, a hybrid algorithm combining the method of moments with the Kirchhoff Approximation is developed. This approach presents overcomes the problem of inaccuracy when using the first-order Kirchhoff Approximation in some degree due to the fact that the scattered fields from the upper rough sea surface is solved by the MOM. The advantage of this hybrid method is performed in the numerical results compared with that by KA. Finally, the influence of the relative permittivity, the height rms and the correlative length, the average heights between the two interfaces on the bistatic scattering coefficient is discussed in detail. It is remained for us to calculate the scattering from two-layer lossy dielectric rough surface using this hybrid method which has more significance.

#### REFERENCES

1. Wismann, V., M. Gade, W. Alpers, and H. Hühnerfuss, "Radar signatures of marine mineral oil spills measured by an airborne multi-radar," *Int. J. Remote Sens.*, Vol. 19, No. 3, 3607–3623, 2005.
2. Blumberg, D. G., et al., "Soil moisture assessment by an airborne scatterometer in Chernobyl disaster area and Negev Desert," *IGARSS 2000, IEEE 2000 International*, Vol. 5, 2011–2013, 2000.
3. Chen, K.-S., A. K. Fung, J. C. Shi, and H.-W. Lee, "Intepretation of backscattering mechanisms from non-Gaussian correlated randomly rough surfaces," *J. of Electromagn. Waves and Appl.*, Vol. 20, No. 1, 105–118, 2006.
4. Fung, A. K. and N. C. Kuo, "Backscattering from multi-scale and exponentially correlated surfaces," *J. of Electromagn. Waves and Appl.*, Vol. 20, No. 1, 3–11, 2006.
5. Sanchez-Gil, J. A., A. A. Maradudin, J. Q. Lu, and V. D. Freilikher, "New features in the transmission of light through thin metal films with randomly rough surfaces," *Geoscience and Remote Sensing Symposium*, Vol. 1, 273–276, 1994.
6. Ho, M., "Scattering of electromagnetic waves from vibrating perfect surfaces: simulation using relativistic boundary conditions," *J. of Electromagn. Waves and Appl.*, Vol. 20, No. 4, 425–433, 2006.

7. Pinel, N. and C. Bourlier, "Modeling of the bistatic electromagnetic scattering from sea surfaces covered in oil for microwave applications," *IEEE Transactions on Geoscience and Remote Sensing*, Vol. 46, No. 2, 385–392, 2008.
8. Ren, Y.-C. and L.-X. Guo, "Study on the multiple scattering and shadowing effect from the two-dimensional rough surface," *Systems Engineering and Electronics*, Vol. 28, No. 4, 496–507, 2006.
9. Guo, L.-X. and Z.-S. Wu, "Fractal characteristics investigation of electromagnetic scattering from 2D conducting rough surface," *Acta Physica Sinica*, Vol. 49, No. 6, 1065–1069, 2000.
10. Fuks, I. M. and A. Voronovitch, "Wave diffraction by rough interfaces in an arbitrary plane-layered medium," *Waves in Random Media*, Vol. 10, S253–S272, 2000.
11. Pinel, N. and C. Bourlier, "Scattering from very rough layers under the geometric optics approximation: Further investigation," *Journal of the Optical Society of America A*, Vol. 25, No. 6, 1293–1306, 2008.
12. Déchamps, N. C., et al., "Numerical simulations of scattering from one-dimensional rough interfaces," *Proceedings. 2003 IEEE International*, Vol. 1, 118–120, 2003.
13. Ogilvy, J. A., *Theory of Wave Scattering from Random Rough Surface*, IOP Publishing, Bristol, 1991.
14. Thorsos, E., "The validity of the Kirchhoff approximation for rough surface scattering using a Gaussian roughness spectrum," *J. Acoust. Soc. Am.*, Vol. 83, 78–91, 1988.
15. Beckman, P. and A. Spizzichino, *The Scattering of Electromagnetic Waves from Rough Surface*, Pergamon, London, 1963.
16. Wang, X., C.-F. Wang, and Y.-B. Gan, "Electromagnetic scattering from a circular target above or below rough surface," *Progress In Electromagnetics Research*, PIER 40, 207–227, 2003.
17. Tsang, L., J. A. Kong, and K. H. Ding, *Scattering of Electromagnetic Waves*, John Wiley & Sons, Inc., United States of America, 2001.